NEUTRON STAR MERGER

Swift and *NuSTAR* observations of GW170817: Detection of a blue kilonova

P. A. Evans,[1]* S. B. Cenko,[2,3] J. A. Kennea,[4] S. W. K. Emery,[5] N. P. M. Kuin,[5] O. Korobkin,[6] R. T. Wollaeger,[6] C. L. Fryer,[6] K. K. Madsen,[7] F. A. Harrison,[7] Y. Xu,[7] E. Nakar,[8] K. Hotokezaka,[9] A. Lien,[10,11] S. Campana,[12] S. R. Oates,[13] E. Troja,[2,14] A. A. Breeveld,[5] F. E. Marshall,[2] S. D. Barthelmy,[2] A. P. Beardmore,[1] D. N. Burrows,[4] G. Cusumano,[15] A. D'Aì,[15] P. D'Avanzo,[12] V. D'Elia,[16,17] M. de Pasquale,[18] W. P. Even,[6,19] C. J. Fontes,[6] K. Forster,[7] J. Garcia,[7] P. Giommi,[17] B. Grefenstette,[7] C. Gronwall,[4,20] D. H. Hartmann,[21] M. Heida,[7] A. L. Hungerford,[6] M. M. Kasliwal,[22] H. A. Krimm,[23,24] A. J. Levan,[13] D. Malesani,[25] A. Melandri,[12] H. Miyasaka,[7] J. A. Nousek,[4] P. T. O'Brien,[1] J. P. Osborne,[1] C. Pagani,[1] K. L. Page,[1] D. M. Palmer,[26] M. Perri,[16,17] S. Pike,[7] J. L. Racusin,[2] S. Rosswog,[27] M. H. Siegel,[4] T. Sakamoto,[28] B. Sbarufatti,[4] G. Tagliaferri,[12] N. R. Tanvir,[1] A. Tohuvavohu[4]

With the first direct detection of merging black holes in 2015, the era of gravitational wave (GW) astrophysics began. A complete picture of compact object mergers, however, requires the detection of an electromagnetic (EM) counterpart. We report ultraviolet (UV) and x-ray observations by *Swift* and the *Nuclear Spectroscopic Telescope Array* of the EM counterpart of the binary neutron star merger GW170817. The bright, rapidly fading UV emission indicates a high mass (≈0.03 solar masses) wind-driven outflow with moderate electron fraction (Y_e ≈ 0.27). Combined with the x-ray limits, we favor an observer viewing angle of ≈30° away from the orbital rotation axis, which avoids both obscuration from the heaviest elements in the orbital plane and a direct view of any ultrarelativistic, highly collimated ejecta (a γ-ray burst afterglow).

At 12:41:04.45 on 17 August 2017 (universal time is used throughout this work), the Laser Interferometer Gravitational-Wave Observatory (LIGO) and Virgo Consortium (LVC) registered a strong gravitational wave (GW) signal (LVC trigger G298048) (*1*), later named GW 170817 (*2*). Unlike previous GW sources reported by LIGO, which involved only black holes (*3*), the gravitational strain waveforms indicated a merger of two neutron stars. Binary neutron star mergers have long been considered a promising candidate for the detection of an electromagnetic counterpart associated with a GW source.

Two seconds later, the Gamma-Ray Burst Monitor (GBM) on the *Fermi* spacecraft triggered on a short (duration, ≈2 s) γ-ray signal consistent with the GW localization, GRB 170817A (*4*, *5*). The location of the *Swift* satellite (*6*) in its low-Earth orbit meant that the GW and γ-ray burst (GRB) localizations were occulted by Earth (*7*) and so not visible to its Burst Alert Telescope. These discoveries triggered a worldwide effort to find, localize, and characterize the EM counterpart (*8*). We present ultraviolet (UV) and x-ray observations conducted as part of this campaign; companion papers describe synergistic efforts at radio (*9*) and optical/near-infrared (*10*) wavelengths.

Search for a UV and x-ray counterpart

Swift began searching for a counterpart to GW170817 with its X-Ray Telescope (XRT) and UV/Optical Telescope (UVOT) at 13:37 (time since the GW and GRB triggers, Δt = 0.039 days). At the time, the most precise localization was from the *Fermi*-GBM (90% containment area of 1626 deg^2), so we imaged a mosaic with radius ~1.1° centered on the most probable GBM position. Subsequently, at 17:54 (Δt = 0.2 days) a more precise localization became available from the LIGO and Virgo GW detectors, with a 90% containment area of only 33.6 deg^2 (*11*). Following the strategy outlined in (*12*), *Swift* began a series of short (120 s) exposures centered on known galaxies in the GW localization (Fig. 1) (*7*).

No new, bright [x-ray flux (f_X) ≥ 10^{-12} erg cm^{-2} s^{-1}] x-ray sources were detected in the wide-area search (XRT imaged 92% of the distance-weighted GW localization) (*7*). In order to quantify the likelihood of recovering any rapidly fading x-ray emission, we simulated 10,000 short GRB afterglows based on a flux-limited sample of short GRBs (*13*) and randomly placed them in the three-dimensional (3D) (distance plus sky position) GW localization, weighted by the GW probability. We found that in 65% of these simulations, we could recover an x-ray afterglow with our wide-area tiling observations (*7*).

At 01:05 on 18 August 2017 (Δt = 0.5 days), a candidate optical counterpart, Swope Supernova Survey 17a (SSS17a) (*14*, *15*), was reported in the galaxy NGC 4993 [distance (d) ≈ 40 Mpc]. Ultimately, this source, which we refer to as EM 170817, was confirmed as the electromagnetic counterpart to the GW detection and the *Fermi* GRB (*8*), making it the closest known short GRB to Earth. Follow-up observations of EM 170817 (*7*) with *Swift* began at 03:34 (Δt = 0.6 days) and with the *Nuclear Spectroscopic Telescope Array* (*NuSTAR*) (*16*) at 05:25 (Δt = 0.7 days). In the first exposures (Δt = 0.6 days), the UVOT detected a bright fading UV source at the location of EM 170817 (Fig. 2). The initial magnitude was $u = 18.19^{+0.09}_{-0.08}$ mag (AB), but subsequent exposures revealed rapid fading at UV wavelengths. The rapid decline in the UV is in contrast to the optical and near-infrared emission, which remained flat for a much longer period of time (Fig. 3) (*10*).

Neither the *Swift*-XRT nor *NuSTAR* instruments detected x-ray emission at the location of EM 170817. A full listing of the *Swift*-XRT and *NuSTAR* upper limits at this location is provided in table S2.

The UV counterpart rules out an on-axis afterglow

In the standard model of GRBs (*17*, *18*), the prompt γ-ray emission is generated by internal processes in a highly collimated, ultrarelativistic jet. As the ejecta expand and shock heat the circumburst medium, electrons are accelerated and

[1]University of Leicester, X-ray and Observational Astronomy Research Group, Leicester Institute for Space and Earth Observation, Department of Physics and Astronomy, University Road, Leicester LE1 7RH, UK. [2]Astrophysics Science Division, NASA Goddard Space Flight Center, Greenbelt, MD 20771, USA. [3]Joint Space-Science Institute, University of Maryland, College Park, MD 20742, USA. [4]Department of Astronomy and Astrophysics, The Pennsylvania State University, University Park, PA 16802, USA. [5]University College London, Mullard Space Science Laboratory, Holmbury St. Mary, Dorking RH5 6NT, UK. [6]Center for Theoretical Astrophysics, Los Alamos National Laboratory, Los Alamos, NM 87545 USA. [7]Cahill Center for Astronomy and Astrophysics, California Institute of Technology, 1200 East California Boulevard, Pasadena, CA 91125, USA. [8]The Raymond and Beverly Sackler School of Physics and Astronomy, Tel Aviv University, Tel Aviv 69978, Israel. [9]Center for Computational Astrophysics, Simons Foundation, 162 5th Avenue, New York, NY 10010, USA. [10]Center for Research and Exploration in Space Science and Technology (CRESST) and NASA Goddard Space Flight Center, Greenbelt, MD 20771, USA. [11]Department of Physics, University of Maryland, Baltimore County, 1000 Hilltop Circle, Baltimore, MD 21250, USA. [12]Istituto Nazionale di Astrofisica (INAF)–Osservatorio Astronomico di Brera, Via Bianchi 46, I-23807 Merate, Italy. [13]Department of Physics, University of Warwick, Coventry CV4 7AL, UK. [14]Department of Physics and Astronomy, University of Maryland, College Park, MD 20742-4111, USA. [15]INAF–Istituto di Astrofisica Spaziale e Fisica Cosmica Palermo, via Ugo La Malfa 153, I-90146, Palermo, Italy. [16]INAF–Osservatorio Astronomico di Roma, via Frascati 33, I-00040 Monteporzio Catone, Italy. [17]Space Science Data Center–Agenzia Spaziale Italiana (ASI), I-00133 Roma, Italy. [18]Department of Astronomy and Space Sciences, University of Istanbul, Beyzt 34119, Istanbul, Turkey. [19]Department of Physical Sciences, Southern Utah University, Cedar City, UT 84720, USA. [20]Institute for Gravitation and the Cosmos, The Pennsylvania State University, University Park, PA 16802, USA. [21]Kinard Lab of Physics, Department of Physics and Astronomy, Clemson University, Clemson, SC 29634–0978, USA. [22]Division of Physics, Mathematics and Astronomy, California Institute of Technology, Pasadena, CA 91125, USA. [23]Universities Space Research Association, 7178 Columbia Gateway Drive, Columbia, MD 21046, USA. [24]National Science Foundation, 2415 Eisenhower Avenue, Alexandria, VA 22314, USA. [25]Dark Cosmology Centre, Niels Bohr Institute, University of Copenhagen, Juliane Maries Vej 30, DK-2100 Copenhagen Ø, Denmark. [26]Los Alamos National Laboratory, B244, Los Alamos, NM 87545, USA. [27]The Oskar Klein Centre, Department of Astronomy, AlbaNova, Stockholm University, SE-106 91 Stockholm, Sweden. [28]Department of Physics and Mathematics, Aoyama Gakuin University, Sagamihara, Kanagawa, 252-5258, Japan.
*Corresponding author. Email: pae9@leicester.ac.uk

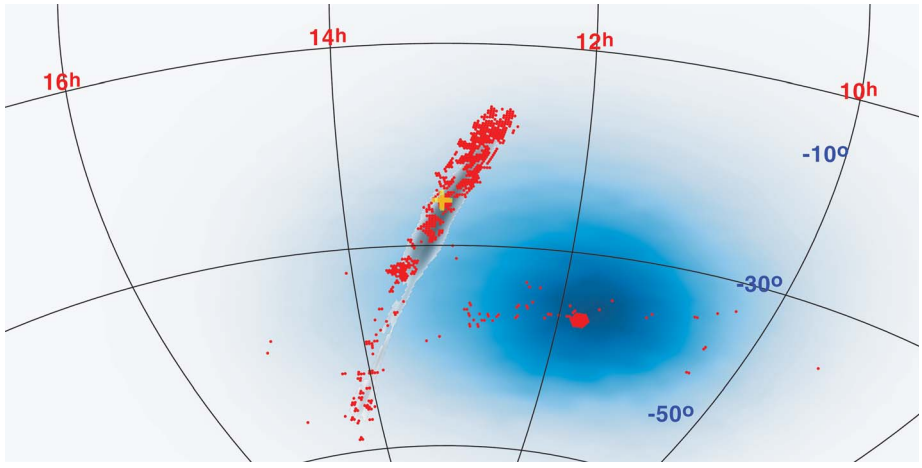

Fig. 1. Skymap of *Swift* XRT observations, in equatorial (J2000) coordinates. The gray probability area is the GW localization (*52*), the blue region shows the *Fermi*-GBM localization, and the red circles are *Swift*-XRT fields of view. UVOT fields are colocated with a field of view 60% of the XRT. The location of the counterpart, EM 170817, is marked with a large yellow cross. The early 37-point mosaic can be seen, centered on the GBM probability. The widely scattered points are from the first uploaded observing plan, which was based on the single-detector GW skymap. The final observed plan was based on the first three-detector map (*11*); however, we show here the higher-quality map (*52*) so that our coverage can be compared with the final probability map [which was not available at the time of our planning (*7*)].

emit a broadband synchrotron afterglow. Our UV and x-ray observations place strong constraints on the presence and/or orientation of such ejecta after GW170817.

In Fig. 4, we plot the median and 25 to 75% distribution of short GRB afterglows (*13*), scaled to the distance of NGC 4993. Although a handful of short GRBs have extremely fast-fading afterglows (*19*) that would have been missed by our observations, the bulk of the population would have been easily detectable (*7*).

We can translate these x-ray upper limits to physical constraints by using the standard analytic afterglow formulation for synchrotron emission (*7*). We found that for on-axis viewing geometries, our nondetections limit the amount of energy coupled to relativistic ejecta (E_{AG}) to be $E_{AG} < \sim 10^{50}$ erg (assuming the energy is radiated isotropically). To verify this result, we ran a series of simulations using the afterglow light curve code BOXFIT (*20*). Over the range of circumburst densities and afterglow energies inferred for short GRBs (*21*), we calculated the x-ray flux at the time of our first *NuSTAR* epoch (which provides the tightest constraints, given typical afterglow decay rates). The results are shown in Fig. 4, yielding a similar constraint ($<\sim 10^{50}$ erg) on the afterglow energy as our analytic approach.

Our x-ray upper limits also help to rule out an afterglow origin for the UV emission: the optical–to–x-ray spectral index $\beta_{OX} \geq 1.6$ at $\Delta t = 0.6$ days is highly inconsistent with observed GRB afterglows (*22*). Analysis of the UV/optical spectral energy distribution (SED) at early times ($\Delta t \leq 2$ days) further supports this conclusion (*7*). Fitting the SED with a blackbody function yields a temperature $T_{BB}(\Delta t = 0.06 \text{ days}) = 7300 \pm 200$ K, and $T_{BB}(\Delta t = 1.0 \text{ day}) = 6400 \pm 200$ K (Fig. 3). A power-law model, as would be expected for synchrotron afterglow radiation, provides a very poor fit to the data (*7*). We therefore conclude that the observed UV counterpart must arise from a different physical process than an on-axis GRB afterglow.

Given the apparent absence of energetic, ultrarelativistic material along the line of sight, the detection of a short GRB is somewhat puzzling. The isotropic γ-ray energy release of GRB 170817A, $E_{\gamma,iso} = (3.08 \pm 0.72) \times 10^{46}$ erg, is several orders of magnitude below any known short GRB (*23*). But even by using the observed correlation (*13*) between $E_{\gamma,iso}$ and x-ray afterglow luminosity, the predicted x-ray flux at $\Delta t = 0.06$ days is still above our *Swift* and *NuSTAR* upper limits.

This requires an alternative explanation for the observed γ-ray emission, such as a (typical) short GRB viewed (slightly) off-axis, or the emission from a cocoon formed by the interaction of a jet with the merger ejecta (*24*–*26*). We return to this issue below in the context of late-time ($\Delta t > \sim 10$ days) x-ray emission (*9*, *10*).

Implications of the early UV emission

Although inconsistent with ultrarelativistic ejecta (such as a GRB afterglow), our UVOT observations nonetheless imply an ejecta velocity that is a substantial fraction of the speed of light (c). If we convert the effective radii derived in our SED fits (Fig. 3) to average velocities, $\bar{v} \equiv R_{BB}/\Delta t$ (R_{BB} is the radius of the emitting photosphere, Δt is the time delay between the trigger and the SED), we find that $\bar{v}(\Delta t = 0.06 \text{ days}) \approx 0.3c$, and $\bar{v}(\Delta t = 1.0 \text{ day}) \approx 0.2c$ (*27*, *28*). These velocities are

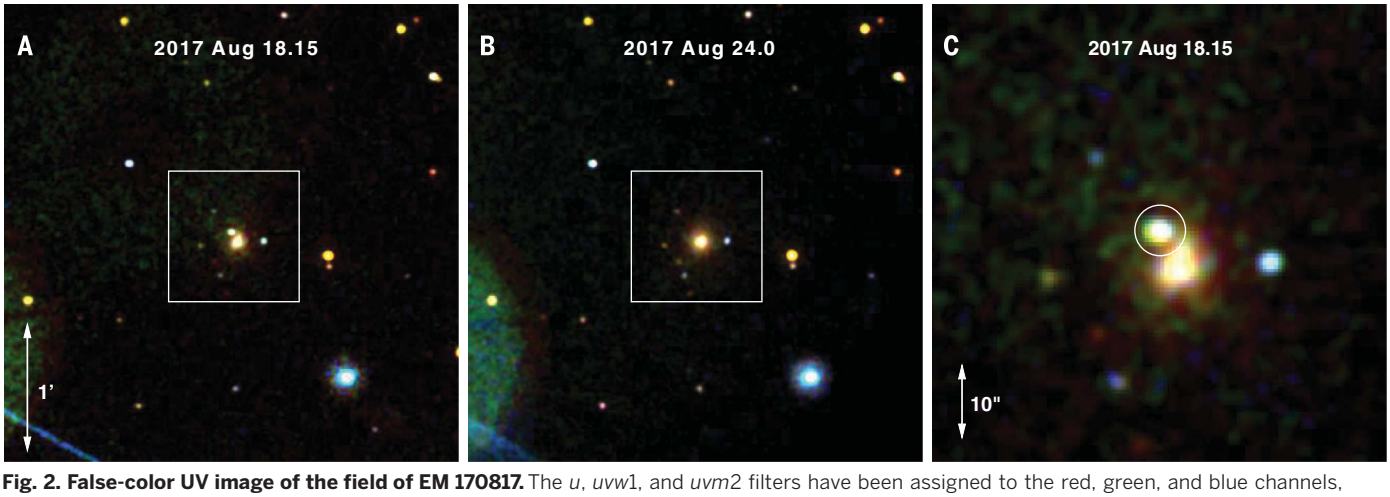

Fig. 2. False-color UV image of the field of EM 170817. The *u*, *uvw*1, and *uvm*2 filters have been assigned to the red, green, and blue channels, respectively. (**A**) Bright UV emission is clearly detected in our first epoch, which (**B**) rapidly fades at blue wavelengths. (**C**) A zoom-in of the first epoch with the transient circled. All images are oriented with north up and east to the left.

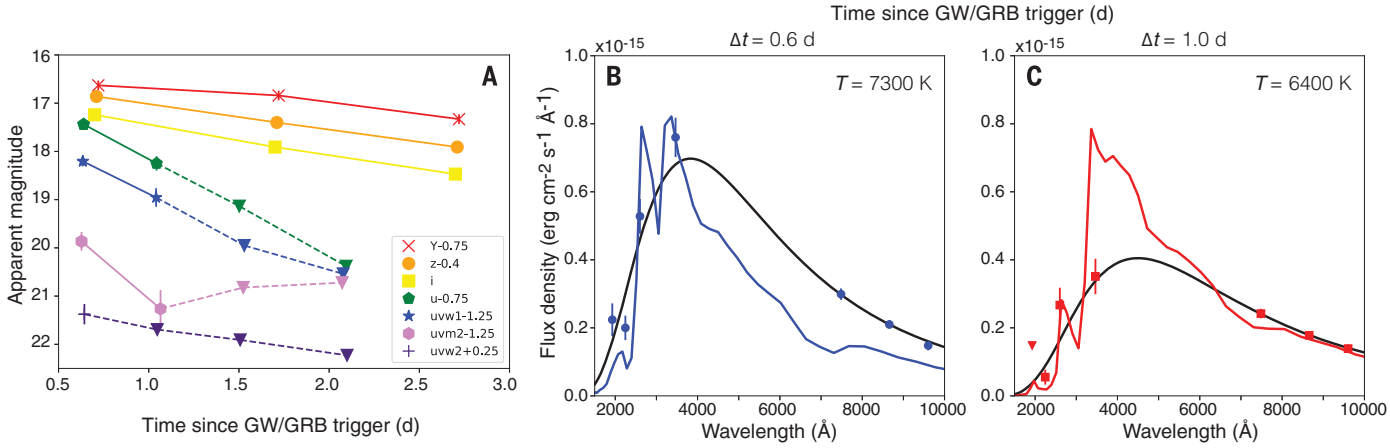

Fig. 3. UV and optical light curves and SEDs. (**A**) *Swift*-UVOT light curve of the optical counterpart EM 170817 of GW170817. The data are corrected for host galaxy contamination. Upper limits are plotted as inverted triangles. Also shown are host-subtracted optical and near-infrared photometry from Pan-STARRS (*53*). (**B** and **C**) The spectral energy distribution of EM 170817, with blackbody models (black curves) demonstrating the rapid cooling of the ejecta. Overplotted are the best-fitting kilonova models (colored lines), in which the wind ejecta have mass 0.03 $M_\odot$ and velocity 0.08*c*, whereas the dynamical ejecta have mass 0.013 $M_\odot$ and velocity 0.3*c* (*7*). The red triangle in (C) is a 3σ upper limit.

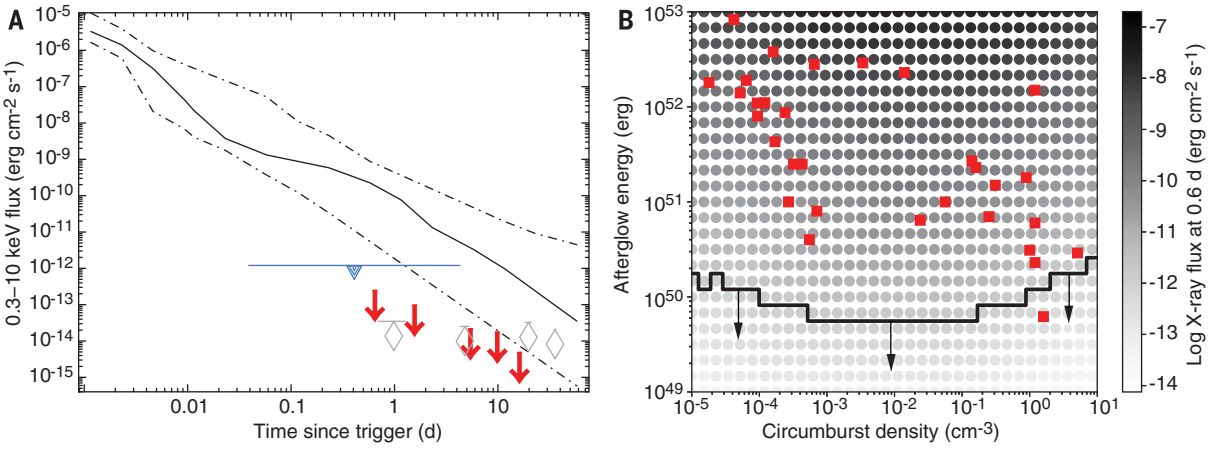

Fig. 4. Predicted x-ray flux of an afterglow to GW170817. (**A**) The distribution of short GRB light curves (*13*), scaled to 40 Mpc. The solid line shows the median behavior; the two dashed-dotted lines represent the 25 and 75 percentiles. The blue line with the triangle corresponds to the time range covered by the large-scale tiling with *Swift*-XRT and shows the typical sensitivity achieved per tile. The red arrows represent the XRT upper limits on emission from EM 170817 obtained by summing all the data up to the time of the arrow. The gray diamonds show the *NuSTAR* limits on emission from EM 170817. (**B**) The x-ray flux predicted for an on-axis jet for a range of isotropic afterglow energies and circumburst densities. The black line indicates the flux upper limit of the first *NuSTAR* observation; red squares are known short GRBs with E_{AG} and n_0 (*21*). Our observations rule out an energetic, ultrarelativistic outflow with $E_{AG} > \sim 10^{50}$ erg for on-axis geometries.

much larger than seen in even the fastest known supernova explosions (*29*). Similarly, the rapid cooling of the ejecta, resulting in extremely red colors at $\Delta t \geq 1$ day (Fig. 3), is unlike the evolution of any common class of extragalactic transient (*30*).

Both of these properties are broadly consistent with theoretical predictions for electromagnetic counterparts to binary neutron star mergers known as kilonovae (sometimes called macronovae or mini supernovae) (*31*, *32*). Numerical simulations of binary neutron star mergers imply that these systems can eject ~10^{-3} to 10^{-2} solar masses ($M_\odot$) of material with velocity (v) ~ 0.1 to 0.2*c*, either via tidal stripping and hydrodynamics at the moment of contact [hereafter referred to as dynamical ejecta (*33*)] or by a variety of processes after the merger, which include viscous, magnetic, or neutrino-driven outflows from a hypermassive neutron star (if this is at least the temporary postmerger remnant) and accretion disc (*34*–*37*). All of these postmerger outflows are expected to have a less neutron-rich composition than the dynamical ejecta, and in this study, we use the general term "winds" to refer to them collectively.

Next, we examined the implications of the relatively bright UV emission at early times. Such UV emission is not a generic prediction of all kilonova models; large opacity in the ejecta owing to numerous atomic transitions of lanthanide elements can suppress UV emission, even at early times (*38*, *39*). This is particularly true for the dynamical ejecta, in which a large fraction of the matter is thought to be neutron-rich [electron fraction (Y_e) ≤ 0.2] and so produces high–atomic number elements (with ~126 neutrons) via rapid neutron capture [the *r*-process (*40*)].

In contrast to the dynamical ejecta, a wind can have a substantially larger electron fraction, particularly if irradiated by neutrinos. Y_e values of ~0.2 have been inferred from accretion discs around rapidly spinning black holes (*41*), whereas a long-lived hypermassive neutron star may increase the neutrino flux even further (Y_e ~ 0.3) (*35*). As a result of these large electron fractions, nucleosynthesis is expected to stop at the second or even first *r*-process peak (elements with 82 or 50 neutrons respectively), resulting in few (if any) lanthanide elements and a dramatically reduced opacity.

Our x-ray nondetections place limits on the presence of a long-lived hypermassive neutron

star (7). In particular, we can rule out any plausible neutron star remnant with a strong magnetic field that lived past the time of our first *Swift* and *NuSTAR* observations (which would effectively be a stable remnant, given the viscous time scale of the accretion disc). Nonetheless, a short-lived or low–magnetic field hypermassive neutron star or a rapidly spinning black hole would both be consistent with our results.

To investigate the plausibility of a wind origin for the early UV emission, we have produced a series of 2D models, varying the ejecta properties (mass, velocity, and composition) (7, 42). We assume that the tidal ejecta are more neutron-rich ($Y_e \approx 0.04$) than the wind ejecta ($Y_e \approx 0.27$ to 0.37) and produce a sizable fraction of lanthanides that obscure the optical and UV emission. The spatial distribution of this high-opacity ejecta is based on merger models (43). Obscuration by the disc formed from this high-opacity material causes a viewing-angle effect (42).

In order to reproduce the early UV emission, we require models with a wind ejecta mass >~0.03 $M_\odot$. Furthermore, a modest electron fraction ($Y_e \approx 0.27$), with substantial amounts of elements from the first *r*-process peak, is strongly favored over larger Y_e ejecta ($Y_e \approx 0.37$, corresponding to mostly Fe-peak elements).

The presence of bright UV emission strongly constrains the observer viewing angle of the binary neutron star merger. Sight lines in the plane of the merger are expected to exhibit dramatically reduced UV emission because of the presence of the Lanthanide-rich dynamical ejecta. For a wind mass (M_{wind}) ≈ 0.03 $M_\odot$, a viewing angle of θ_{obs} < ~30° with respect to the rotation axis is preferred. Orientations up to ~40° can be accommodated with $M_{wind} \approx 0.1\ M_\odot$; at larger viewing angles, the wind ejecta mass becomes unphysically large.

Although the wind component can provide a good fit to the UV emission, on its own it underpredicts the observed optical/near-infrared flux at this time. Adding dynamical ejecta with $M_{dyn} \approx 0.01\ M_\odot$ and $v \approx 0.3c$ can provide a reasonable fit to the early SEDs (Fig. 3). However, we emphasize that the properties of the dynamical ejecta are only poorly constrained at early times; analysis of the full optical/near-infrared light curve is necessary for accurate constraints on the Lanthanide-rich material (10).

Although much of the γ-ray emission generated during the *r*-process is reradiated at optical/near-infrared wavelengths, it may also be possible to directly observe emission lines from β-decay in the *NuSTAR* bandpass. We have calculated the expected signal from 10 to 100 keV for a range of ejecta masses, and it is well below the *NuSTAR* limits for GW170817 (7).

The above modeling of the kilonova emission assumes that the merger ejecta is unaffected by any energetic jet (or that no such jet is formed). For jets with a narrow opening angle (θ_{jet} < 10°), numerical simulations (24) have shown that any such jet-ejecta interaction will have negligible effects on the observed light curves on the time scales probed by our observations.

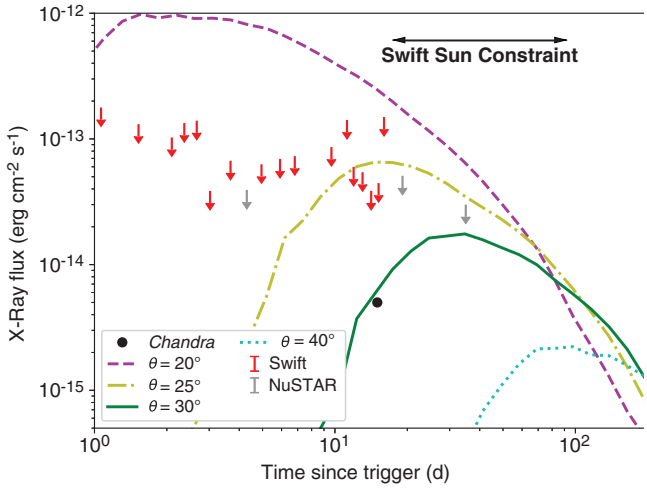

Fig. 5. Simulated x-ray afterglow light curves for typical short GRB parameters. Here, E_{AG} = 2×10^{51} erg, $n_0 = 5 \times 10^{-3}$ cm^{-3}, and θ_{jet} = 0.2 rad; the true values of these parameters are uncertain and vary between GRBs (20). Curves are shown for a range of viewing angles, with the *Swift*-XRT and *NuSTAR* limits marked. An off-axis orientation of ≈30° is consistent with both the early *Swift*-XRT and *NuSTAR* limits and the recently reported *Chandra* detection (44). The anticipated peak time will occur when *Swift* and *Chandra* cannot observe the field because of proximity to the Sun.

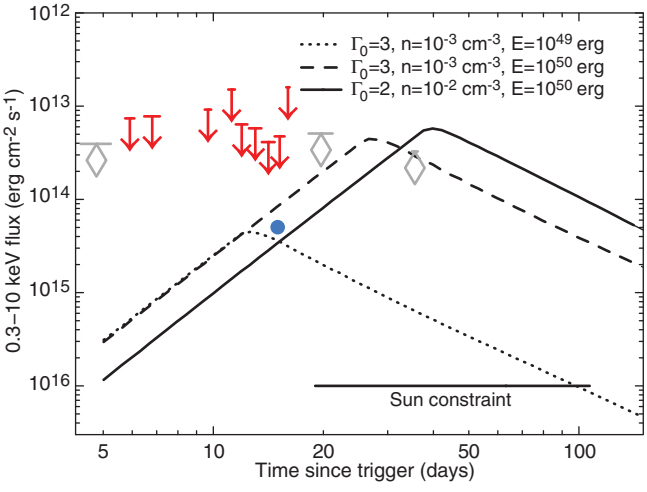

Fig. 6. Predicted x-ray light curves from a mildly relativistic jet. The jet is based on model predictions (24), for a range of different values for the inital bulk Lorentz factor of the cocoon (Γ_0), circumburst density (*n*), and cocoon energy (*E*). Data points are the *Swift*-XRT (red arrows) and *NuSTAR* (gray diamonds) upper limits and the *Chandra* detection (blue) of EM 170817. The range of plausible peak times is not observable by *Swift* (or *Chandra*).

However, if the jet opening angle were sufficiently large, the energy from this jet (and the resulting cocoon) may accelerate material in the merger ejecta to mildly relativistic velocities. Numerical simulations in our companion paper (10) offer some support for this scenario, providing a reasonable fit to the temperature and bolometric luminosity evolution of EM 170817. However, they lack the detailed radiation transport calculations presented here.

Late-time x-ray emission: Off-axis jet or cocoon

Although no x-ray emission at the location of EM 170817 was detected by *Swift* or *NuSTAR*, a faint x-ray source was detected by *Chandra* at $\Delta t \approx 9$ days (44), although the flux was not initially reported. Subsequent *Chandra* observations at $\Delta t \approx 15$ days reported luminosity (L_X) ≈ 9×10^{38} erg s^{-1} (45, 46). A variety of models predict long-lived x-ray emission at a level >~10^{40} erg s^{-1} after the merger of two neutron stars. For example, (quasi-)isotropic x-ray emission may be expected because of prolonged accretion onto a black hole remnant, or from the spin-down power of a long-lived hypermassive neutron star. These models are not consistent with the *Swift* or *NuSTAR* limits or the *Chandra* flux (7), suggesting that if a magnetar formed after the merger event, it collapsed to a black hole before our first x-ray observation (within 0.6 days of formation).

A possible explanation for the late-time x-ray emission is an off-axis (orphan) afterglow (47). If the binary neutron star merger produces a collimated, ultrarelativistic jet, initially no emission will be visible to observers outside the jet opening angle. As the outflow decelerates, the relativistic beaming becomes weaker, and the jet spreads laterally, illuminating an increasing fraction of the sky. Off-axis observers can expect to see rising emission until the full extent of the jet is visible, at which point the decay will appear similar to that measured by on-axis observers. Simulations of such events showed that starting a few days after the merger, off-axis afterglows

represent the dominant population of GW counterparts detectable by *Swift* (*48*).

We ran a series of simulations using the BOXFIT code (*20*) to use our x-ray limits and the reported *Chandra* detections to constrain the orientation of GW170817 (*7*). For the median values of short GRB afterglow energy ($E_{AG} = 2 \times 10^{51}$ erg), circumburst density ($n_0 = 5 \times 10^{-3}$ cm^{-3}), and jet opening angle [$\theta_{jet} = 0.2$ rad (12°)] (*21*), the resulting light curves are plotted in Fig. 5. With the *Swift* and *NuSTAR* nondetections, these models rule out any viewing angle with $\theta_{obs} < \sim 20°$. Assuming the emission reported by *Chandra* results from an orphan afterglow, we infer $\theta_{obs} \approx 30°$.

This inferred orientation is entirely consistent with the results of our analysis of the early UV emission. However, it is difficult to simultaneously explain the observed γ-ray emission in this scenario because it would require a viewing angle only slightly outside the jet edge (*10*). Either the observed GRB 170817A is powered by a source distinct from this jet, or we are forced to disfavor an orphan afterglow model for the late-time x-ray emission.

Alternatively, delayed x-ray emission may result if the initial outflow speed is mildly relativistic, as would be expected from models in which propagation in the merger ejecta forms a hot cocoon around the jet (*24*). In this case, the rise is dictated by the time necessary for the cocoon to sweep up enough material in the circumburst medium to radiate efficiently; this in turn depends on the energy carried by the expanding cocoon, its bulk Lorentz factor, and the circumburst density. Shown in Fig. 6 are x-ray light curves predicted by this model for a range of plausible values of these parameters, along with the x-ray limits from *NuSTAR* and *Swift*-XRT and the *Chandra* detection (*45*, *46*). The latest *NuSTAR* datapoint disfavors energetic cocoon models, particularly those at high density. But lower-energy or -density models can fit all the x-ray data while simultaneously accounting for the γ-ray emission (*10*).

Our inferences regarding the origin of the late-time x-ray emission are broadly consistent with the conclusions reached in our companion radio paper (*9*). Both an orphan afterglow and a mildly relativistic cocoon model make specific predictions for the evolution of the broadband flux over the upcoming months after the merger (Figs. 5 and 6) (*9*).

Conclusions

The discovery of a short GRB simultaneous with a GW binary neutron star merger represents the start of a new era of multimessenger astronomy. It confirms that binary neutron star mergers can generate short γ-ray transients (*49*), although the connection to classical short GRBs remains unclear. Furthermore, GW170817 provides robust evidence that *r*-process nucleosynthesis occurs in the aftermath of a binary neutron star merger (*10*).

Although a kilonova detection after a short GRB has been previously reported (*50*, *51*), our multiwavelength data set has allowed us to confront kilonova models with UV and x-ray observations. The absence of x-ray emission largely rules out the presence of an energetic, ultrarelativistic, and collimated outflow viewed from within the opening angle of the jet. The late-time x-ray emission is consistent with a collimated, ultrarelativistic outflow viewed at an off-axis angle of ≈30° (an orphan afterglow). A mildly relativistic outflow, as may be expected if the jet were enveloped by a hot cocoon, is also consistent with our x-ray data [and may naturally explain the peculiar properties of the γ-ray emission (*10*)].

The presence of bright, rapidly fading UV emission was not a generic prediction of kilonova models and requires special circumstances to avoid obscuration by the heavy elements formed in the dynamical ejecta. We found that we can reproduce the early UV and optical emission with a massive ($M \approx 0.03\ M_{\odot}$) and high-velocity ($v \approx 0.08c$) outflow comprising moderate-Y_e (first *r*-process peak) material at a viewing angle of ≈30°; such winds may be expected if the remnant is a relatively long-lived hypermassive neutron star or a rapidly spinning black hole. Alternatively, if the hot cocoon is able to accelerate material in the ejecta to mildly relativistic speeds, this may also be able to account for the early UV emission (*10*).

REFERENCES AND NOTES

1. The LIGO Scientific Collaboration, the Virgo Collaboration, *Gamma Ray Coordinates Network Circular* 21505 (2017).
2. The LIGO Scientific Collaboration, the Virgo Collaboration, *Phys. Rev. Lett.* 10.1103/PhysRevLett.119.161101 (2017).
3. B. P. Abbott *et al.*, *Phys. Rev. X* **6**, 041015 (2016).
4. V. Connaughton *et al.*, *Gamma Ray Coordinates Network Circular* 21506 (2017).
5. A. Goldstein, *Astrophys. J.* **848**, 10.3847/2041-8213/aa8f41 (2017).
6. N. Gehrels *et al.*, *Astrophys. J.* **611**, 1005–1020 (2004).
7. Materials and methods are available as supplementary materials.
8. B. P. Abbott *et al.*, *Astrophys. J.* **848**, 10.3847/2041-8213/aa91c9 (2017).
9. G. Hallinan *et al.*, *Science* **358**, 1579–1583 (2017).
10. M. M. Kasliwal *et al.*, *Science* **358**, 1559–1565 (2017).
11. The LIGO Scientific Collaboration, the Virgo Collaboration, *Gamma Ray Coordinates Network Circular* 21513 (2017).
12. P. A. Evans *et al.*, *Mon. Not. R. Astron. Soc.* **462**, 1591–1602 (2016).
13. P. D'Avanzo *et al.*, *Mon. Not. R. Astron. Soc.* **442**, 2342–2356 (2014).
14. D. Coulter *et al.*, *Gamma Ray Coordinates Network Circular* 21529 (2017).
15. D. A. Coulter *et al.*, *Science* **358**, 1556–1558 (2017).
16. F. A. Harrison *et al.*, *Astrophys. J.* **770**, 103 (2013).
17. P. Meszaros, M. J. Rees, *Astrophys. J.* **405**, 278 (1993).
18. T. Piran, *Rev. Mod. Phys.* **76**, 1143–1210 (2004).
19. A. Rowlinson *et al.*, *Mon. Not. R. Astron. Soc.* **409**, 531–540 (2010).
20. H. van Eerten, A. van der Horst, A. MacFadyen, *Astrophys. J.* **749**, 44 (2012).
21. W. Fong, E. Berger, R. Margutti, B. A. Zauderer, *Astrophys. J.* **815**, 102 (2015).
22. A. J. van der Horst *et al.*, *Astrophys. J.* **699**, 1087–1091 (2009).
23. B. P. Abbott *et al.*, *Astrophys. J.* **848**, 10.3847/2041-8213/aa920c (2017).
24. O. Gottlieb, E. Nakar, T. Piran, arXiv:1705.10797 [astro-ph.HE] (2017).
25. D. Lazzati, A. Deich, B. J. Morsony, J. C. Workman, *Mon. Not. R. Astron. Soc.* **471**, 1652–1661 (2017).
26. A. Kathirgamaraju, R. Barniol Duran, D. Giannios, arXiv:1708.07488 [astro-ph.HE] (2017).
27. D. Malesani, D. Watson, J. Hjorth, *Gamma Ray Coordinates Network Circular* 21577 (2017).
28. P. Cowperthwaite, M. Nicholl, E. Berger, *Gamma Ray Coordinates Network Circular* 21578 (2017).
29. M. Modjaz, Y. Q. Liu, F. B. Bianco, O. Graur, *Astrophys. J.* **832**, 108 (2016).
30. P. S. Cowperthwaite, E. Berger, *Astrophys. J.* **814**, 25 (2015).
31. L.-X. Li, B. Paczynski, *Astrophys. J.* **507**, L59–L62 (1998).
32. B. D. Metzger, *Living Rev. Relativ.* **20**, 3 (2017).
33. S. Rosswog *et al.*, *Astron. Astrophys.* **341**, 499 (1999).
34. B. D. Metzger, A. L. Piro, E. Quataert, *Mon. Not. R. Astron. Soc.* **396**, 304–314 (2009).
35. A. Perego *et al.*, *Mon. Not. R. Astron. Soc.* **443**, 3134–3156 (2014).
36. D. Martin *et al.*, *Astrophys. J.* **813**, 2 (2015).
37. O. Just, A. Bauswein, R. A. Pulpillo, S. Goriely, H.-T. Janka, *Mon. Not. R. Astron. Soc.* **448**, 541–567 (2015).
38. D. Kasen, N. R. Badnell, J. Barnes, *Astrophys. J.* **774**, 25 (2013).
39. J. Barnes, D. Kasen, *Astrophys. J.* **775**, 18 (2013).
40. E. M. Burbidge, G. R. Burbidge, W. A. Fowler, F. Hoyle, *Rev. Mod. Phys.* **29**, 547–650 (1957).
41. R. Fernández, D. Kasen, B. D. Metzger, E. Quataert, *Mon. Not. R. Astron. Soc.* **446**, 750–758 (2015).
42. R. T. Wollaeger *et al.*, arXiv:1705.07084 [astro-ph.HE] (2017).
43. S. Rosswog, O. Korobkin, A. Arcones, F.-K. Thielemann, T. Piran, *Mon. Not. R. Astron. Soc.* **439**, 744–756 (2014).
44. E. Troja, L. Piro, T. Sakamoto, B. Cenko, A. Lien, *Gamma Ray Coordinates Network Circular* 21765 (2017).
45. E. Troja *et al.*, *Nature* 10.1038/nature24290 (2017).
46. D. Haggard *et al.*, *Astrophys. J.* **848**, 10.3847/2041-8213/aa8ede (2017).
47. J. E. Rhoads, *Astrophys. J.* **525**, 737–749 (1999).
48. P. A. Evans *et al.*, *Mon. Not. R. Astron. Soc.* **455**, 1522–1537 (2016).
49. D. Eichler, M. Livio, T. Piran, D. N. Schramm, *Nature* **340**, 126–128 (1989).
50. N. R. Tanvir *et al.*, *Nature* **500**, 547–549 (2013).
51. E. Berger, W. Fong, R. Chornock, *Astrophys. J.* **774**, L23 (2013).
52. The LIGO Scientific Collaboration, the Virgo Collaboration, *Gamma Ray Coordinates Network Circular* 21527 (2017).
53. S. Smartt *et al.*, *Nature* 10.1038/nature24303 (2017).

ACKNOWLEDGMENTS

We acknowledge the leadership and scientific vision of Neil Gehrels (1952–2017), former principal investigator of *Swift*, without whom the work we present here would not have been possible. Funding for the *Swift* mission in the United Kingdom is provided by the UK Space Agency. S.R.O. gratefully acknowledges the support of the Leverhulme Trust Early Career Fellowship. The *Swift* team at the Mission Operations Center at The Pennsylvania State University acknowledges support from NASA contract NAS5-00136. The Italian *Swift* team acknowledges support from ASI-INAF grant I/004/11/3. S.R. has been supported by the Swedish Research Council (VR) under grant 2016- 03657_3, by the Swedish National Space Board under grant Dnr. 107/16, and by the research environment grant "Gravitational Radiation and Electromagnetic Astrophysical Transients (GREAT)" funded by the Swedish Research council (VR) under grant Dnr 2016- 06012. This research used resources provided by the Los Alamos National Laboratory Institutional Computing Program, which is supported by the U.S. Department of Energy National Nuclear Security Administration under contract DE-AC52-06NA25396. Very Large Telescope data were obtained under European Southern Observatory program number 099.D-0668. *NuSTAR* acknowledges funding from NASA contract NNG08FD60C. A.J.L. and N.R.T. acknowledge funding from the European Research Council under the European Union's Horizon 2020 program, grant 725246. Researchers at Los Alamos National Laboratory were supported by the National Nuclear Security Administration of the U.S. Department of Energy under contract DE-AC52-06NA25396. S.W.K.E. is supported by a Science and Technology Facilities Council studentship. The observations are archived at www.swift.ac.uk for *Swift* and https://heasarc.gsfc.nasa.gov/docs/nustar/nustar_archive.html for *NuSTAR*, under the observation IDs given in table S2. Reduced photometry and surveyed areas are tabulated in the supplementary materials. The BOXFIT software is available at http://cosmo.nyu.edu/afterglowlibrary/boxfit2011.html, SuperNu at https://bitbucket.org/drrossum/supernu/wiki/Home, and access to WinNet source code and input files will be granted upon request via https://bitbucket.org/korobkin/winnet. The dynamical model ejecta are available at http://compact-merger.astro.su.se/downloads_fluid_trajectories.html (as run 12). The SuperNu and BOXFIT input files are available in the supplementary materials.

SUPPLEMENTARY MATERIALS

www.sciencemag.org/content/358/6370/1565/suppl/DC1
Materials and Methods
Figs. S1 to S6
Tables S1 to S3
References (*54–120*)
Simulation Input Files

14 September 2017; accepted 4 October 2017
Published online 16 October 2017
10.1126/science.aap9580

Science

Swift and *NuSTAR* observations of GW170817: Detection of a blue kilonova

P. A. Evans, S. B. Cenko, J. A. Kennea, S. W. K. Emery, N. P. M. Kuin, O. Korobkin, R. T. Wollaeger, C. L. Fryer, K. K. Madsen, F. A. Harrison, Y. Xu, E. Nakar, K. Hotokezaka, A. Lien, S. Campana, S. R. Oates, E. Troja, A. A. Breeveld, F. E. Marshall, S. D. Barthelmy, A. P. Beardmore, D. N. Burrows, G. Cusumano, A. D'Aì, P. D'Avanzo, V. D'Elia, M. de Pasquale, W. P. Even, C. J. Fontes, K. Forster, J. Garcia, P. Giommi, B. Grefenstette, C. Gronwall, D. H. Hartmann, M. Heida, A. L. Hungerford, M. M. Kasliwal, H. A. Krimm, A. J. Levan, D. Malesani, A. Melandri, H. Miyasaka, J. A. Nousek, P. T. O'Brien, J. P. Osborne, C. Pagani, K. L. Page, D. M. Palmer, M. Perri, S. Pike, J. L. Racusin, S. Rosswog, M. H. Siegel, T. Sakamoto, B. Sbarufatti, G. Tagliaferri, N. R. Tanvir and A. Tohuvavohu

Science **358** (6370), 1565-1570.
DOI: 10.1126/science.aap9580originally published online October 16, 2017

GROWTH observations of GW170817

The gravitational wave event GW170817 was caused by the merger of two neutron stars (see the Introduction by Smith). In three papers, teams associated with the GROWTH (Global Relay of Observatories Watching Transients Happen) project present their observations of the event at wavelengths from x-rays to radio waves. Evans *et al.* used space telescopes to detect GW170817 in the ultraviolet and place limits on its x-ray flux, showing that the merger generated a hot explosion known as a blue kilonova. Hallinan *et al.* describe radio emissions generated as the explosion slammed into the surrounding gas within the host galaxy. Kasliwal *et al.* present additional observations in the optical and infrared and formulate a model for the event involving a cocoon of material expanding at close to the speed of light, matching the data at all observed wavelengths.

Science, this issue p. 1565, p. 1579, p. 1559; see also p. 1554